ISSN 0022-4766, Journal of Structural Chemistry, 2023, Vol. 64, No. 12, pp. 2438-2450. © Pleiades Publishing, Ltd., 2023.
Russian Text © The Author(s), 2023, published in Zhurnal Strukturnoi Khimii, 2023, Vol. 64, No. 12, 121572.

NANO-SIZED COPPER FILMS PREPARED BY MAGNETRON SPUTTERING

V. S. Sulyaeva[1]*, V. R. Shayapov[1], M. M. Syrokvashin[1], A. K. Kozhevnikov[1], and M. L. Kosinova[1]

Copper films with a thickness varying from 6 nm to 100 nm are prepared by magnetron sputtering. The films are characterized by homogeneous and fine-grained microstructure. The X-ray diffraction data confirm formation of a copper fcc phase orientated predominantly in the (111) direction. Depending on the growth conditions, the size of Cu grains in the films varies from 7 nm to 20 nm. The refractive index of the films increases from 0.52 to 1.22 with decreasing copper film thickness. The transmittance of the films decreases as their thickness increases from 6 nm to 62 nm, and the transparency of the films with the same thickness decreases with increasing sputtering power and decreasing argon flow rate. The surface resistivity of the films decreases from 8.89±0.06 Ω/sq to 1.47±0.01 Ω/sq as their thickness increases from 20 nm to 70 nm.

DOI: 10.1134/S0022476623120156

Keywords: thin copper films, magnetron sputtering, optical properties, surface resistivity.

INTRODUCTION

Formation of thin copper films is interesting from scientific and technical viewpoints due to the possibility of using these materials in numerous technological applications. Copper exhibits a number of outstanding properties such as high melting point and electrical conductivity, good thermal conductivity, plasticity, wear resistance, etc.[1-3]. Submicron thick copper films with nanosized grain are employed in micro- and nanoelectronics, catalysis, biomedicine, production of sensors and electromagnetic devices, etc. [4-7]. Possessing a number of advantages of copper over aluminum (lower resistivity, resistance to electromigration, higher cell switching speeds), copper is currently viewed as the main material of conductive intercell connectors in integrated circuits [4, 8]. Ultrathin (<10 nm) copper films, combining high transmittance with good electrical conductivity, may be promising transparent electrodes in solar cells, LEDs, and other photovoltaic devices [9, 10]. The multi-purpose use of copper films, optimization of their structural and functional characteristics, and expansion of their functionality constantly pose new synthesis challenges. That is the reason why the study of Cu film deposition has been considered an important task for more than half a century by now. At the same time, researchers have met troubles when trying to obtain films with desired structural parameters required to control their functional characteristics and ensure their reproducibility. Copper films are usually prepared on Si(100), glass, and quartz glass substrates using chemical vapor deposition [11-16], atomic layer deposition [17, 18], physical vapor deposition (magnetron sputtering, electron-beam

[1]Nikolaev Institute of Inorganic Chemistry, Siberian Branch, Russian Academy of Sciences, Novosibirsk, Russia; *veronica@niic.nsc.ru. Original article submitted September 28, 2023; revised October 20, 2023; accepted October 24, 2023.

 0022-4766/23/6412-2438 © 2023 by Pleiades Publishing, Ltd.

evaporation, thermal evaporation) [4, 19, 20], and electrochemical deposition [21, 22]. When choosing the preparation method, requirements for the deposited films should be taken into account. The most important of them include good adhesion to the substrate surface, uniform thickness, homogeneity, grain fineness, and lack of porosity.

In recent years, magnetron sputtering has established itself as one of the most promising methods for producing thin copper films. High-purity, uniform, and highly adhesive films can be prepared by this method at high deposition rates while (and most importantly) preserving stable deposition conditions and precise control for the thickness and grain size of Cu films. The tasks approached by researchers concern the effect of thickness, structure, and grain size of films on their physical characteristics. The properties of deposited films (deposition rate, surface morphology, roughness, microstructure, electrical, mechanical, and optical characteristics) are determined by deposition conditions such as reaction chamber geometry, magnetron discharge parameters (current, voltage, and sputtering power), pressure of the working gas (argon), presence of additional gas (e.g., hydrogen), distance between the Cu target and the substrate, and the substrate temperature. Currently, the main attention is focused on the synthesis of nano-sized copper films. Most of reported works consider the influence of various synthesis parameters and film thicknesses on electrical properties of the films. The works devoted to optical and mechanical characteristics of thin Cu films are few in number. The deposition of Cu targets by magnetron sputtering is usually performed at room temperature. The dependence of the properties of films prepared by this method on temperature has been considered only in few sporadic works. The effect of deposition conditions on the properties of copper films is illustrated by the data in Table 1.

According to publications, electrical conductivity values, mechanical characteristics, and optical constants of copper films depend on their structure, surface morphology, and thickness. There are several works devoted to the influence of synthesis parameters on the rate of copper film formation. It was reported that the rate of film deposition decreases with increasing Cu target - substrate distance in the reaction chamber and increases with increasing sputtering power or p(Ar) [25, 32]. Particular attention was paid to the effect of deposition conditions on the structural properties and morphological characteristics of films. It was established that the grain size and the root mean square roughness of the film surface increases with increasing film thickness [26, 32-34], while the crystallinity of the films improves [26]. Note that the average crystallite size significantly increases with increasing temperature. The authors of [27] reported that the grain size increased from 10 nm to 123 nm as T_{depos} increased from 250 °C to 400 °C. According to [23-25], the film surface becomes rougher and their structure changes from fine-grained to columnar with increasing argon pressure.

The design and optimization of devices and instruments require data on the functional characteristics of thin copper films. Special attention is paid to the dependence of film resistivity on magnetron sputtering parameters and film thickness. As the thickness increases, the conductive properties of films improve, while the resistivity rapidly decreases and then approaches some constant value, usually exceeding the 1.67 μΩ·cm value typical for bulk materials [26, 35-37]. High resistivity of ultrathin films is explained by the presence of impurities (oxygen, carbon etc.) and by the presence of defects and strains in the films [28, 29]. Note that the conductive layer is formed only in the films thicker than 5 nm [38].

Optical constants of copper films (refractive index n and extinction coefficient k) were determined by ellipsometric studies. The data on the study and simulation of optical constants of solid copper were reported earlier in [39-44]. However, there is much less data related to optical constants of thin copper films, particularly to their dependence on deposition conditions. Determining true constants of metal films by indirect ellipsometry is difficult due to some innate features of this method, which will be discussed below. Additional information on the effect of deposition conditions on the optical properties of copper films can be obtained by transmission spectrophotometry. The few studies devoted to the Cu film transparency were focused on its dependence on film thickness, and we could find no data related to the effect of other magnetron sputtering parameters. The authors of [26] showed that the transmittance of Cu films exceeds 90% at a film thickness of 2-3 nm and decreases abruptly to 76-80% as the film thickness increases to 3.5 nm. According to the ellipsometry data, the refractive index of films changes from 1.38 to 1.95 with increasing copper film thickness [30].

TABLE 1. Synthesis Conditions and Properties of Copper Films Prepared by Magnetron Sputtering of a Cu Target in Argon

Synthesis method	Deposition conditions		Properties of Cu films					Ref.
	T_{depos}, °C l, cm P, W	p, mTorr F(Ar), cm^3/min	d_{Cu}, nm V, nm/min	Rms, nm D, nm	ρ, μΩ·cm	H, GPa E, GPa	T, % n	
MPP MS	RT 10 2000	0.8-5.3 80	1200-1700 44-82	2.2-6.4 –	–	2.6-3.4 128-147	– –	[23], [24]
DC MS	RT 25-55 500	0.5-3.0 –	– 6-32	0.8-3.0 –	–	– –	– –	[25]
RF MS	RT 6.5 17	1.5 60	2-250 3	0.2-0.5 2.4-6.0	5000-25	– –	40-90 (d_{Cu} = 2-10 nm) –	[26]
RF MS	250, 400 7 –	7.5 –	532, 596 10	– 10, 123	38.4, 2.2	– –	– –	[27]
DC MS	RT 5 160	7.5-15 –	18-222 50	– 6-24	–	– –	– –	[28]
DC MS	RT 2.3-2.9 –	3.8 –	5-2000 5-50	– 1-24	3-8.5	– –	– –	[29]
RF MS	RT – 300	1 30	4.5-17.0 –	0.7-1.9 –	39-8.9	– –	– 1.38-1.95	[30]
DC MS	RT – –	38 –	13-28 7.2	– 9.2-21.3	–	– –	10-40 –	[31]

Note. Deposition temperature (T_{depos}), target - substrate distance (l); plasma power (P); reactor's working pressure (p); argon flow rate (F(Ar)); film thickness (d_{Cu}); deposition rate (V); grain size (D); resistivity (ρ); hardness (H); elastic modulus (E); transmittance (T); refractive index (n). Modulated pulsed power magnetron sputtering system (MPPMS); direct current magnetron sputtering (DC MS); radio frequency magnetron sputtering (RF MS).

Thus, it is an interesting task to develop a technique for depositing thin copper films by magnetron sputtering, to study the kinetics of metal layer growth and structural properties of the films, and to determine the effect of deposition parameters on electrical and optical properties of obtained films.

EXPERIMENTAL

The copper films were prepared in a Torus 2″ HV magnetron sputtering system (Fig. 1) using a Cu target (99.99 wt.% purity) as the cathode and Ar (high-purity grade) as the working gas. Polished quartz glass and Si(100) plates were used as the substrates for Cu film deposition. Before the experiments, the substrates were degreased. Then, the silicon plates were additionally chemically etched. Copper targets were sputtered using an APEL-M-1.5PDC-800-2 direct current generator in the constant power mode. Before the film deposition procedure, the system was pumped out to the residual pressure of $3 \cdot 10^{-5}$ Torr. The constant rate of Ar flow during the deposition was maintained using a Horiba SEC-Z512 flow

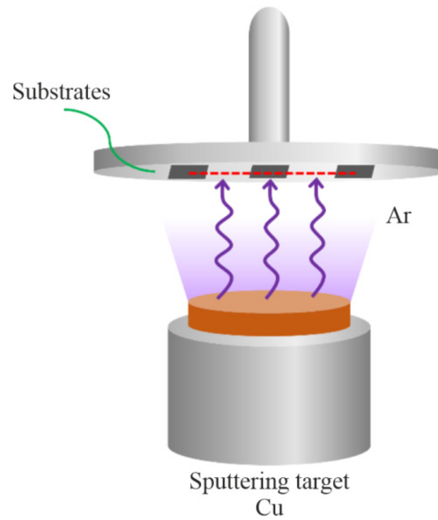

Fig. 1. Schematic experimental technique.

controller. The working pressure in the vacuum chamber was (2-4)·10^{-3} Torr. The substrates were not additionally heated during the deposition.

The influence of deposition parameters on the film properties were studied in the course of three series of experiments. When preparing films of various thicknesses, the sputtering time was varied at a constant power and an argon flow rate. The dependence of film properties on the generator power and the argon flow rate was determined using films of the same thickness. The experimental conditions are listed in Table 2.

Film characterization methods. The phase composition of the layers was determined by XRD using a Shimadzu XRD-7000 diffractometer (CuK_α radiation; λ = 0.154051 nm; Ni filter; 2θ range: 5-60°; 2θ step: 0.03°; counting time per point: 1 s). Transmission electron microscopy (TEM) and energy dispersive (EDX) elemental mapping images were obtained on a ThemisZ microscope (Thermo Fisher Scientific) at an accelerating voltage of 200 kV using a Super-X EDS detector. Surface morphology was studied on a Jeol JSM 6700F scanning electron microscope, the elemental composition of Cu films was determined using an EDS Bruker Quantax 200 energy dispersive attachment equipped with a X-Flash 6|60 detector. The SEM method was also used to study the transverse fractures of the samples and to determine their thickness. The thickness and optical constants of some films were additionally calculated by the ellipsometry method. The ellipsometric measurements of copper films were performed on a LEF-3M ellipsometer (λ = 632.8 nm) at eight different light incidence angles varied

TABLE 2. Experimental Conditions of Magnetron Sputtering

Conditions	Values									
P, W	100	200	300	300	300	300	300	300	300	300
F(Ar), cm^3/min	50	50	50	25	100	50	50	50	50	50
d_{Cu}, nm	35	30	28	26	27	100	62	43	21	12
$V_{depos,}$ nm/min	35	90	138	140	150	125	128	136	126	144
Target	Cu									
Sputtering power, W	100-300									
Substrates	Si(100), quartz glass									
Substrate - target distance, cm	10									
Residual pressure, Torr	3·10^{-5}									
Ar flow rate, cm^3/min	25-100									
Working pressure, Torr	(2-4)·10^{-3}									
Deposition temperature, °C	22									

from 45° to 80° with a step of 5°. When solving the inverse problem, the searched parameters were the refractive index *n* and the extinction coefficient k. Film thicknesses were determined from the SEM measurements of samples transverse fractures. The inverse ellipsometry problem was solved by minimizing the mean squared error (MSE):

$$MSE = \sqrt{\frac{\sum_{N}^{i=1}[(\psi_{pi} - \psi_{ei})^2 + (\Delta_{pi} - \Delta_{ei})^2]}{2N}}, \quad (1)$$

where ψ_{ei} and Δ_{ei} are the measured values of ellipsometric angles ψ and Δ for the *i*th incident angle; ψ_{pi} and Δ_{pi} are the calculated values of these angles; *N* is the number of incident angles.

The transmittance spectra of the samples on quartz glass substrates was recorded using a spectrophotometric system based on a "Kolibri-2" spectrometer (VMK Optoelektronika, Russia), an AvaLight-DHS combined deuterium-tungsten source (Avantes, Netherlands), a special attachment, and fiber optic cables (Ocean Optics, China).

The surface resistivity of Cu/SiO_2 samples was measured at room temperature by a four-point probe method using a Keysight 34465A voltmeter immediately after removing the samples from the vacuum chamber. The final resistivity value was calculated as the average of 10 independent measurements for each sample.

RESULTS AND DISCUSSION

Copper films with a thickness ranging from 6 nm to 100 nm, depending on the process conditions, were prepared by magnetron sputtering. The deposition rates from 35 nm/min to 150 nm/min were obtained by varying the sputtering parameters. As can be seen from Table 2, the rate of Cu film deposition increases with increasing sputtering power and the Ar flow rate. Similar tendencies were reported earlier in [26, 32].

The samples were structurally characterized by XRD. Fig. 2 shows the XRD patterns of copper films prepared at different sputtering power. All the samples exhibited a reflection at ~43.3° assigned, according to the Inorganic Crystal Structure Database (ICSD), to the (111) plane of the copper cubic modification [45]. The absence of CuO or Cu_2O peaks indicates high purity of the obtained copper layers. The XRD data confirm the formation of crystalline nanoparticles of the fcc copper phase orientated predominantly in the (111) direction [46]. The position of the diffraction peak of copper nanoparticles agrees well with the data reported earlier by other authors [27, 37, 46].

The recorded diffraction peak is broad because of a low crystallinity of the films composed of nanoparticles. The width of this peak increases with increasing sputtering power (Fig. 2*a*). The average size of copper particles was estimated from the Debye–Scherrer equation:

$$D = \frac{0.9\lambda}{\beta\cos\theta},$$

where *D* is the crystallite size; λ is the X-ray wavelength; β is the diffraction peak's width at half height; θ is the diffraction angle. The coherent scattering regions (sizes of crystalline domain) for the prepared copper films are listed in Table 3. The TEM image of copper film (Fig. 2*c*) shows the top layer of the copper film. The interlayer distance is 2.09 Å, which corresponds to the (111) peak of the Cu fcc phase. Fig. 2*d* shows the EDX mapping of a cross-section of the Si/Cu/epoxy layer structure. The thickness of the Cu layer is 50 nm.

Fig. 3 shows the surface morphology of Cu films prepared at different sputtering power. The grain size on the film surface decreases with increasing sputtering power and is accompanied by the broadening of their diffraction peaks. The SEM images of all prepared copper films show the same granular surface morphology with a grain size varying from 8 nm to 20 nm, depending on experimental conditions.

Table 3 lists the average sizes of crystallites and grains of Cu films estimated from the Debye–Scherrer formula and from surface micrographs obtained by XRD and SEM methods. As can be seen, the values obtained by these two methods agree well with each other. The crystallite and grain sizes expectedly increase with increasing film thickness. At the same time, the crystallite and grain sizes are slightly diminished with increasing power and Ar flow rate.

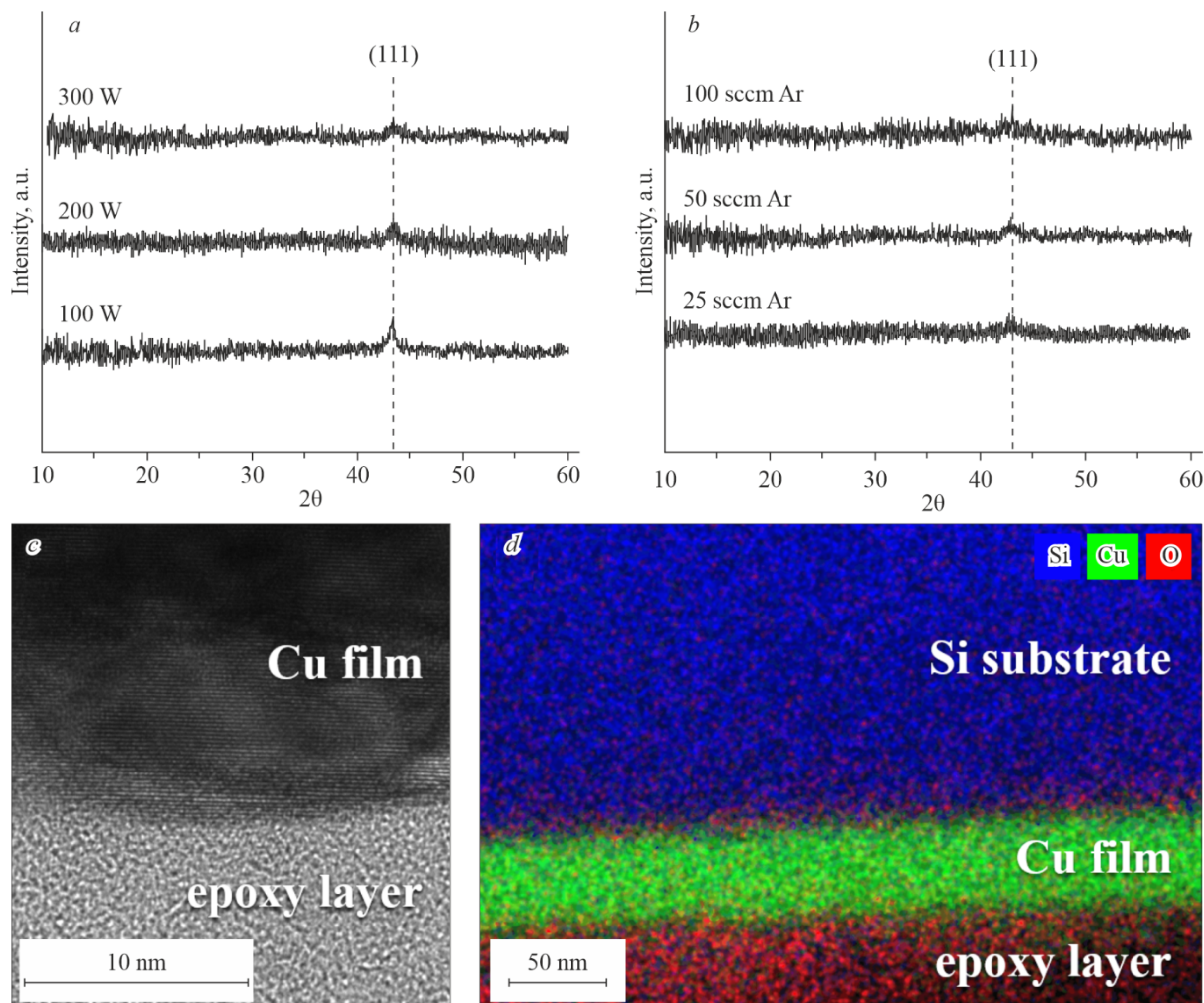

Fig. 2. XRD patterns of Cu films prepared at $F(\text{Ar}) = 50\ \text{cm}^3/\text{min}$ and different sputtering power (*a*) and at 300 W and various Ar flow rates (*b*). TEM image of copper film (*c*) and EDX mapping of silicon, copper, and oxygen in the Si/Cu/epoxy layer structure (*d*).

TABLE 3. Crystallite and Grain Sizes of Cu Films of Various Thicknesses Obtained under Varied Deposition Conditions

P, W	$F(\text{Ar})$, cm^3/min	d_{Cu}, nm	D, nm (XRD)	D, nm (SEM)
100	50	35	11	12
200	50	30	9	10
200	50	80	15	17
300	*50*	28	8	8
300	*25*	28	8	9
300	*100*	25	7	8
300	50	100	20	20
300	50	62	16	17
300	50	43	13	14

We also studied the uniformity of copper deposition over the thickness of the formed layers. Fig. 4 shows the cross-sections of samples prepared by simultaneous deposition of films on three substrates fixed on a holder along a 50 mm long line (dashed line in Fig. 1) so that the distances between the centers of the samples shown in Fig. 4*a* and 4*b* and in Fig. 4*b* and

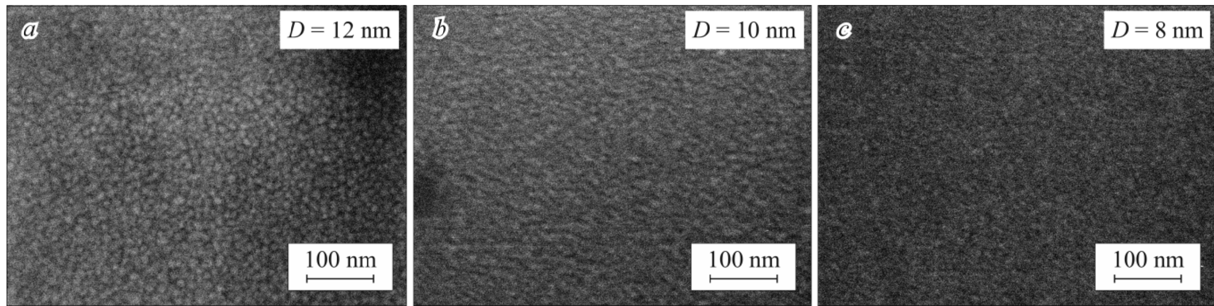

Fig. 3. SEM images of the surfaces of Cu films prepared by magnetron sputtering at a power of 100 W (*a*), 200 W (*b*), and 300 W (*c*).

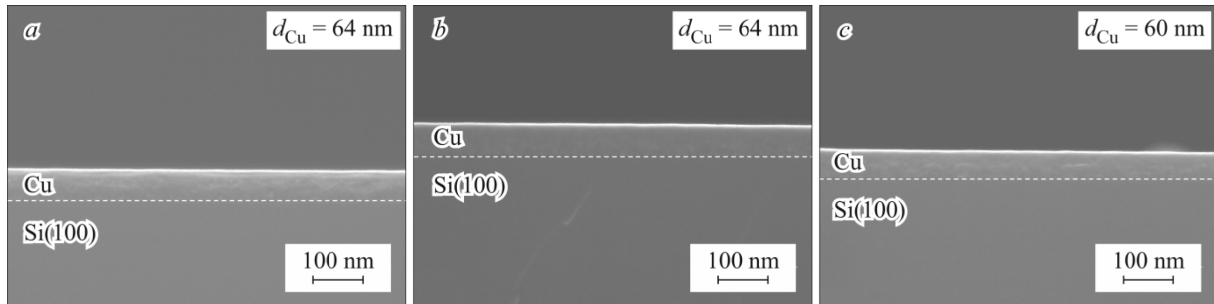

Fig. 4. Cross-section SEM images of Cu/Si(100) samples prepared in the same experiment.

4*c* were 25 mm. The corresponding thicknesses of copper layers are indicated in the micrographs. Thus, it was shown that the uniformity deviation does not exceed 6% at a distance of 50 mm.

According to the ellipsometric data obtained for freshly prepared samples, the refractive indices of the films increase with decreasing film thickness (Table 4). In fact, this effect may be related not only to fundamental properties of the films, but also to the problem of choosing an adequate model for the sample. The factors complicating the choice of a model (roughness, oxide layer on the substrate, interface layer, etc.) become more important for thinner films. When films, especially ultrathin ones, are exposed to air, an inhomogeneous oxide film is formed on their surface as a result of oxidation, thus highly complicating the determination of the film's true optical constants. Note that numerous devoted to experimental measurements and theoretical calculations of copper optical constants [39, 42-44] reported values n = 0.24-0.34, k = 3.2-3.6 for λ = 632.8 nm. At the same time, the authors of other studies observed as high n values as 0.58 [41] and 0.67 [40]. Most of these works considered bulk copper samples, and their characteristics not always correspond to those of thin films whose optical properties are significantly affected by their surface structure and morphology.

In the present work, we studied the influence of deposition conditions on the transmission spectra of the films. The transmission spectra were recorded at 400-900 nm for the samples of different thicknesses (Fig. 5) and for the samples with a similar thickness prepared using different magnetron sputtering power and argon flow rate (Fig. 6).

All the obtained transmission spectra of Cu/quartz glass structures contain a weak broad peak at ~590 nm. Similar results were reported in [19, 26, 31]. The behavior of the transmittance spectrum with increasing copper film thickness

TABLE 4. Optical Constants of Cu Films of Various Thicknesses

P, W	F(Ar), cm^3/min	d_{Cu}, nm	n	k
300	50	43	0.52	2.92
300	50	28	0.58	3.10
300	50	12	1.22	2.78

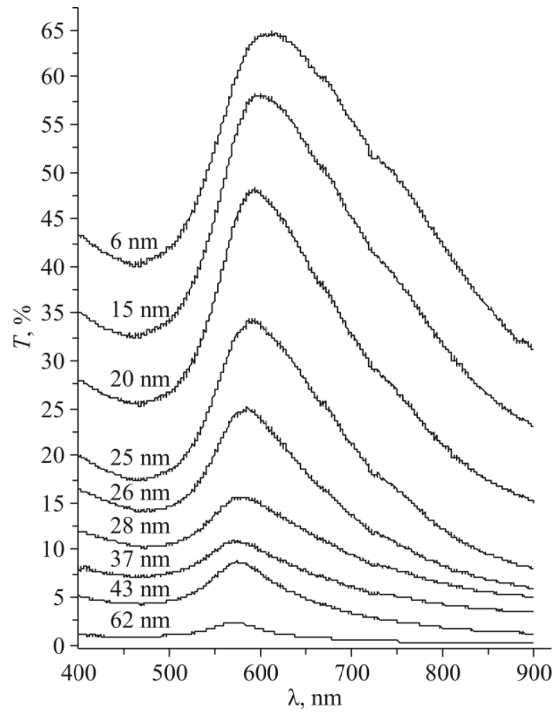

Fig. 5. Optical transmission spectra for copper films of different thicknesses.

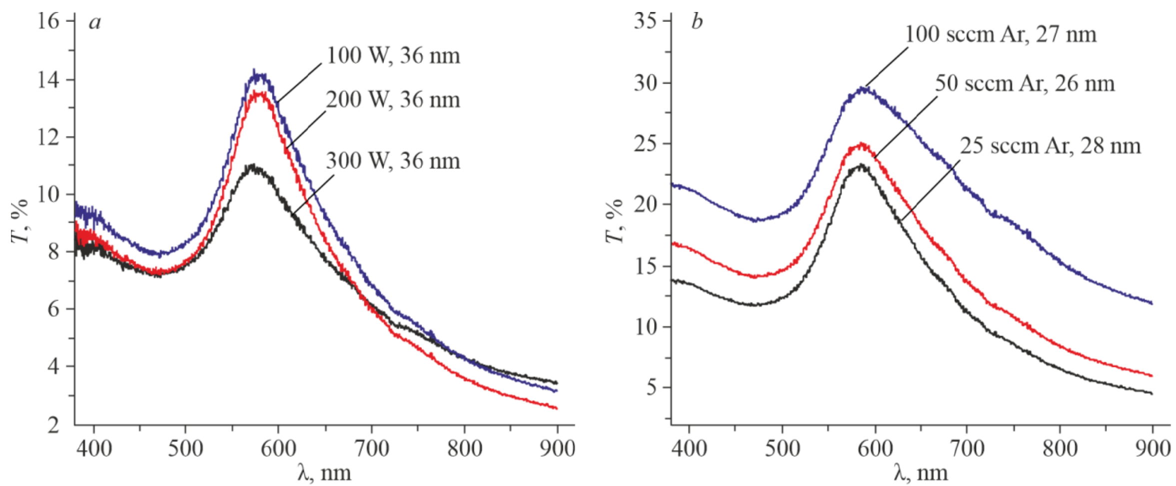

Fig. 6. Optical transmission spectra for different power (*a*) and Ar flow rate (*b*).

(Fig. 5) is typical for absorbing films [31]. At the same time, it was established that the transmission of films of the same thickness diminishes with increasing discharge power and decreasing argon flow rate (Fig. 6).

Our calculations based on the mathematical apparatus of optical thin-film systems showed that the influence of the extinction coefficient on the transmittance for $k \approx 3$ significantly exceeds the influence of the refractive index. Thus, the observed transmittance decrease is due to the absorption increase with increasing power or decreasing the argon flow rate. The fact that typical extinction coefficients of prepared films (Table 4) are smaller than those reported earlier for bulk copper suggests that optical properties of the films become more similar to those of bulk copper as the sputtering power increases or the argon flow rate decreases.

It is known that the surface of thin copper films usually oxidizes upon storage in air after the deposition. In this work, we studied a 33 nm thick Cu film prepared at $F(\mathrm{Ar}) = 50\ \mathrm{cm^3/min}$ and $P = 300$ W, determined the changes of its

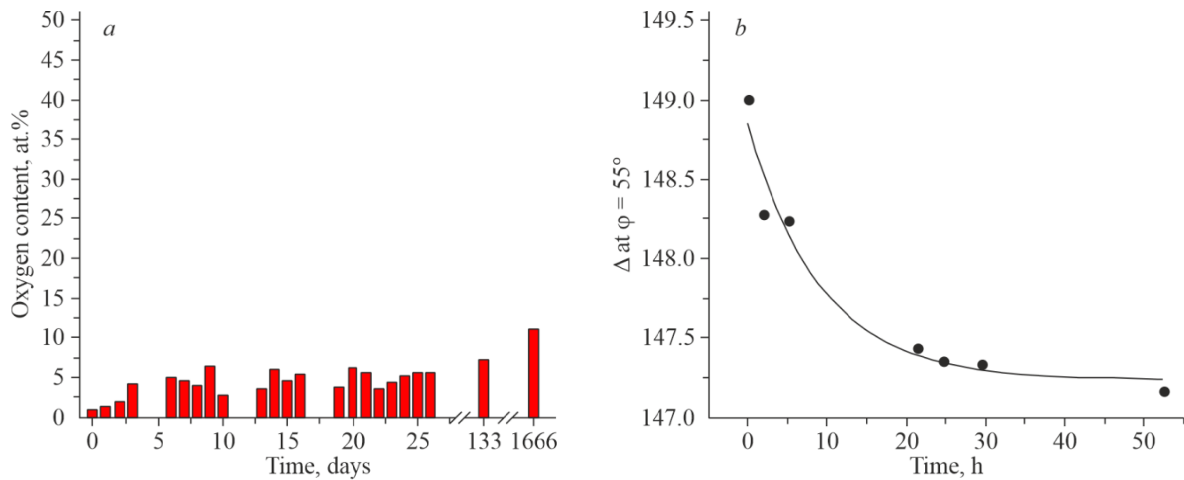

Fig. 7. Time dependence of oxygen concentration in a copper film according to the EDX data (*a*) and Δ angle time dependence (*b*).

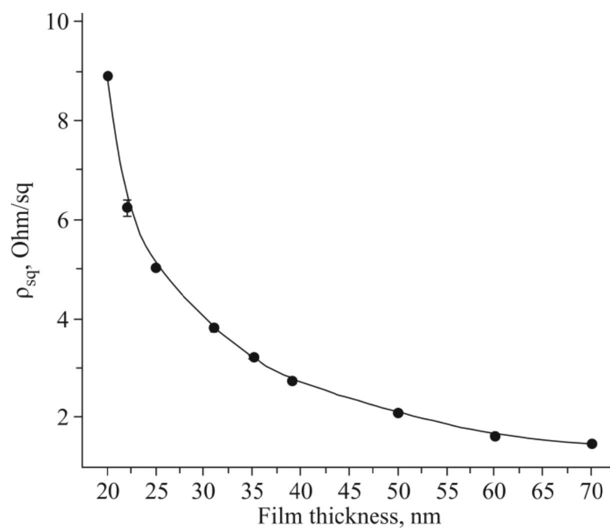

Fig. 8. Surface resistivity of copper films as a function of thickness.

elemental composition by EDX and the changes over time upon storage in air under standard conditions of function ψ and Δ using the ellipsometry method. The diagram in Fig. 7*a* shows changes in the oxygen content in the sample upon a long-term storage (4.5 years or 1666 days). As can be seen, the oxygen content in the freshly deposited film was as small as less than 1 at.%. In the first days of storage, the film gradually oxidized, and the oxygen content increased up to 4-5 at.%. This is also confirmed by the behavior of the ellipsometric parameter Δ which changes abruptly in the first hours and then reaches some constant value (Fig. 7*b*). Thus, the elemental composition of the copper film changes slightly during the first hours of storage and then remains stable for a long time.

It was determined by the measurements of Cu film resistivity that the surface resistivity (ρ_{sq}) of the films decreases abruptly in a nonlinear manner with increasing film thickness and changes only slightly thicknesses exceeding 50 nm (Fig. 8). This dependence indicates that ohmic losses in the prepared samples are decreased due to the increase of grain sizes with increasing film thickness (Table 3). This is due to the fact that increased grain size weakens the scattering of charge carriers at grain boundaries, thus increasing the film conductivity. Note that the character of the revealed dependency and the experimental dependences of film surface resistivity on thickness correlate with the data reported earlier in [27, 46, 47].

CONCLUSIONS

Ultra-thin copper films characterized by a thickness of $6 < d_{Cu} < 100$ nm and a homogeneous and fine-grained microstructure were grown by magnetron sputtering in argon on quartz glass and Si(100) substrates at room temperature. High homogeneity of the formed layers was confirmed by the cross-section SEM images of Cu/Si(100) structures. The XRD and TEM data revealed formation of the fcc phase of copper with a predominant orientation in the (111) direction. The grain size increased with increasing film thickness and decreased with increasing power and argon flow rate. It was determined that optical and electrical properties of ultrathin copper films vary significantly within the studied thickness range. The surface resistivity of the films decreases abruptly from 20 nm to 31 nm. As the film thickness increases still further, the resistivity gradually decreases and then tends to constant value. The obtained values of optical constants n and k may be useful for the design of plasmonic devices based on thin copper films.

FUNDING

The study was funded by the Russian Science Foundation (project No. 23-79-00026, https://rscf.ru/project/23-79-00026/) using facilities of the Shared Research Center "National Center of Investigation of Catalysts" at Boreskov Institute of Catalysis, Siberian Branch of Russian Academy of Sciences.

CONFLICT OF INTERESTS

The authors of this work declare that they have no conflicts of interests.

REFERENCES

1. J. R. Davis. ASM Specialty Handbook: Copper and Copper Alloys. ASM International, **2001**.
2. J. Sarkar. Sputtering Materials for VLSI and Thin Film Devices. William Andrew, **2014**, Chap. 5: Sputtering targets and thin films for integrated circuits, 291-416. https://doi.org/10.1016/b978-0-8155-1593-7.00005-9
3. Y. Cao, Y. Xia, B. Duan, W. Mu, X. Tan, and H. Wu. Microstructure evolution and anti-wear mechanism of Cu film fabricated by magnetron sputtering deposition. *Mater. Lett.*, **2022**, *315*. https://doi.org/10.1016/j.matlet.2022.131941
4. H.-W. Kim. Recent trends in copper metallization. *Electronics*, **2022**, *11*, 2914. https://doi.org/10.3390/electronics 11182914
5. H. Li, P. Wei, D. Gao, and G. Wang. In situ Raman spectroscopy studies for electrochemical CO_2 reduction over Cu catalysts. *Curr. Opin. Green Sustain. Chem.*, **2022**, *34*, 100589. https://doi.org/10.1016/j.cogsc.2022.100589
6. Y. Yin, W. Jing, F. Wang, Y. Liu, and L. Guo. Electro-reduced copper on polymeric C_3N_4 for photocatalytic reduction of CO_2. *Carbon*, **2023**, *214*, 118317. https://doi.org/10.1016/j.carbon.2023.118317
7. S. Rtimi, D. D. Dionysiou, S. C. Pillai, and J. Kiwi. Advances in catalytic/photocatalytic bacterial inactivation by nano Ag and Cu coated surfaces and medical devices. *Appl. Catal., B*, **2019**, *240*, 291-318. https://doi.org/10.1016/j.apcatb. 2018.07.025
8. A. Radisic, O. Lühn, H. G. G. Philipsen, Z. El-Mekki, M. Honore, S. Rodet, S. Armini, C. Drijbooms, H. Bender, and W. Ruythooren. Copper plating for 3D interconnects. *Microelectron. Eng.*, **2011**, *88*, 701-704. https://doi.org/10.1016/ j.mee.2010.06.030
9. S. Lim, D. Han, H. Kim, S. Lee, and S. Yoo. Cu-based multilayer transparent electrodes: A low-cost alternative to ITO electrodes in organic solar cells. *Sol. Energy Mater. Sol. Cells*, **2012**, *101*, 170-175. https://doi.org/10.1016/j.solmat. 2012.01.016

10. P. Xiong, Y. Liu, T. Ding, P. Chen, H. Wang, and Y. Duan. Transparent electrodes based on ultrathin/ultra smooth Cu films produced through atomic layer deposition as new ITO-free organic light-emitting devices. *Org. Electron.*, **2018**, *58*, 18-24. https://doi.org/10.1016/j.orgel.2018.03.036
11. V. N. Vertoprakhov and S. A. Krupoder. Preparation of thin copper films from the vapour phase of volatile copper(I) and copper(II) derivatives by the CVD method. *Usp. Khim.*, **2000**, *69*, 1149-1177. https://doi.org/10.1070/rc2000v069n12abeh000572
12. A. M. Willcocks, T. Pugh, J. A. Hamilton, A. L. Johnson, S. P. Richards, and A. J. Kingsley. CVD of pure copper films from novel iso-ureate complexes. *Dalton Trans.*, **2013**, *42*, 5554-5565. https://doi.org/10.1039/c3dt00104k
13. S. Walke, M. B. Mandake, M. Naniwadekar, R. W. Tapre, T. Ghosh, and Y. Qureshi. A review on copper chemical vapour deposition. *Mater. Today Proc.*, **2023**. https://doi.org/10.1016/j.matpr.2022.12.140
14. N. Bahlawane, P. A. Premkumar, F. Reilmann, K. Kohse-Höinghaus, J. Wang, F. Qi, B. Gehl, and M. Bäumer. CVD of conducting ultrathin copper films. *J. Electrochem. Soc.*, **2009**, *156*, D452. https://doi.org/10.1149/1.3205478
15. J. L. Hodgkinson, D. Massey, and D. W. Sheel. The deposition of copper-based thin films via atmospheric pressure plasma-enhanced CVD. *Surf. Coatings Technol.*, **2013**, *230*, 260-265. https://doi.org/10.1016/j.surfcoat.2013.06.053
16. V. Krisyuk, L. Aloui, N. Prud'Homme, S. Sysoev, F. Senocq, D. Sa□lor, and C. Vahlas. CVD of pure copper films from amidinate precursor. *Electrochem. Solid-State Lett.*, **2011**, *14*, D26. https://doi.org/10.1149/1.3526142
17. K. Bernal Ramos, M. J. Saly, and Y. J. Chabal. Precursor design and reaction mechanisms for the atomic layer deposition of metal films. *Coord. Chem. Rev.*, **2013**, *257*, 3271-3281. https://doi.org/10.1016/j.ccr.2013.03.028
18. Z. Li, A. Rahtu, and R. G. Gordon. Atomic layer deposition of ultrathin copper metal films from a liquid copper(I) amidinate precursor. *J. Electrochem. Soc.*, **2006**, *153*, C787. https://doi.org/10.1149/1.2338632
19. O. Stenzel, S. Wilbrandt, S. Stempfhuber, D. Gäbler, and S.-J. Wolleb. Spectrophotometric characterization of thin copper and gold films prepared by electron beam evaporation: Thickness dependence of the drude damping parameter. *Coatings*, **2019**, *9*, 181. https://doi.org/10.3390/coatings9030181
20. J. Vancea, F. Hofmann, and H. Hoffmann. Grain size-dependent Hall coefficient in polycrystalline copper films. *J. Phys. Condens. Matter*, **1989**, *1*, 7419-7424. https://doi.org/10.1088/0953-8984/1/40/015
21. B. Im, S. Kim, and S.-H. Kim. Nucleation-controlled growth of Cu thin films electrodeposited directly on ALD Ru diffusion barrier in additive-free electrolyte for Cu interconnect. *Microelectron. Eng.*, **2023**, *275*, 111991. https://doi.org/10.1016/j.mee.2023.111991
22. A. I. Vorobjova, V. A. Labunov, E. A. Outkina, and D. V. Grapov. Metallization of vias in silicon wafers to produce three-dimensional microstructures. *Russ. Microelectron.*, **2021**, *50*, 8-18. https://doi.org/10.1134/s1063739721010108/9
23. D. Meng, Y. G. Li, Z. T. Jiang, and M. K. Lei. Stick-climb-slip induced damage mode in Cu/Si(100) thin films deposited by modulated pulsed power magnetron sputtering during scratch. *Vacuum*, **2020**, *174*, 109233. https://doi.org/10.1016/j.vacuum.2020.109233
24. D. Meng, Y. G. Li, Z. T. Jiang, and M. K. Lei. Scratch behavior and FEM modelling of Cu/Si(100) thin films deposited by modulated pulsed power magnetron sputtering. *Surf. Coatings Technol.*, **2019**, *363*, 25-33. https://doi.org/10.1016/j.surfcoat.2019.02.008
25. M. V. Shandrikov, I. D. Artamonov, A. S. Bugaev, E. M. Oks, K. V. Oskomov, and A. V. Vizir. Deposition of Cu-films by a planar magnetron sputtering system at ultra-low operating pressure. *Surf. Coatings Technol.*, **2020**, *389*, 125600. https://doi.org/10.1016/j.surfcoat.2020.125600
26. B. L. Zhu, C. H. Yi, X. Zhao, J. M. Ma, J. Wu, and X. W. Shi. Improvement of transparent conductive properties of Cu films by introducing H_2 into deposition atmosphere during RF magnetron sputtering. *Superlattices Microstruct.*, **2020**, *145*, 106628. https://doi.org/10.1016/j.spmi.2020.106628

27. B. Giroire, M. Ali Ahmad, G. Aubert, L. Teule-Gay, D. Michau, J. J. Watkins, C. Aymonier, and A. Poulon-Quintin. A comparative study of copper thin films deposited using magnetron sputtering and supercritical fluid deposition techniques. *Thin Solid Films*, **2017**, *643*, 53-59. https://doi.org/10.1016/j.tsf.2017.09.002
28. S. K. Mukherjee, L. Joshi, and P. K. Barhai. A comparative study of nanocrystalline Cu film deposited using anodic vacuum arc and dc magnetron sputtering. *Surf. Coatings Technol.*, **2011**, *205*, 4582-4595. https://doi.org/10.1016/j.surfcoat.2011.03.119
29. K. Mech, R. Kowalik, and P. Żabiński. Cu thin films deposited by DC magnetron sputtering for contact surfaces on electronic components. *Arch. Metall. Mater.*, **2011**, *56*, 903-908. https://doi.org/10.2478/v10172-011-0099-4
30. Z. A. Ansari, K. Hong, and C. Lee. Structural and electrical properties of porous silicon with rf-sputtered Cu films. *Mater. Sci. Eng. B*, **2002**, *90*, 103-109. https://doi.org/10.1016/S0921-5107(01)00917-5
31. E. Shahriari and M. Ghasemi Varnamkhasti. Nonlinear optical and electrical characterization of nanostructured Cu thin film. *Superlattices Microstruct.*, **2014**, *75*, 523-532. https://doi.org/10.1016/j.spmi.2014.08.001
32. K.-Y. Chan and B.-S. Teo. Atomic force microscopy (AFM) and X-ray diffraction (XRD) investigations of copper thin films prepared by dc magnetron sputtering technique. *Microelectronics J.*, **2006**, *37*, 1064-1071. https://doi.org/10.1016/j.mejo.2006.04.008
33. K.-Y. Chan, T.-Y. Tou, and B.-S. Teo. Thickness dependence of the structural and electrical properties of copper films deposited by dc magnetron sputtering technique. *Microelectronics J.*, **2006**, *37*, 608-612. https://doi.org/10.1016/j.mejo.2005.09.016
34. D. L. Ma, P. P. Jing, Y. L. Gong, B. H. Wu, Q. Y. Deng, Y. T. Li, C. Z. Chen, Y. X. Leng, and N. Huang. Structure and stress of Cu films prepared by high power pulsed magnetron sputtering. *Vacuum*, **2019**, *160*, 226-232. https://doi.org/10.1016/j.vacuum.2018.11.039
35. H.-D. Liu, Y.-P. Zhao, G. Ramanath, S. Murarka, and G.-C. Wang. Thickness dependent electrical resistivity of ultrathin (< 40 nm) Cu films. *Thin Solid Films*, **2001**, *384*, 151-156. https://doi.org/10.1016/S0040-6090(00)01818-6
36. X. Cui, D. A. Hutt, and P. P. Conway. Evolution of microstructure and electrical conductivity of electroless copper deposits on a glass substrate. *Thin Solid Films*, **2012**, *520*, 6095-6099. https://doi.org/10.1016/j.tsf.2012.05.068
37. B. H. Wu, J. Wu, F. Jiang, D. L. Ma, C. Z. Chen, H. Sun, Y. X. Leng, and N. Huang. Plasma characteristics and properties of Cu films prepared by high power pulsed magnetron sputtering. *Vacuum*, **2017**, *135*, 93-100. https://doi.org/10.1016/j.vacuum.2016.10.032
38. V. A. Vdovin, V. G. Andreev, P. S. Glazunov, I. A. Khorin, and Y. V. Pinaev. Optical coefficients of nanoscale copper films in the range of 9-11 GHz. *Opt. Spectrosc.*, **2019**, *127*, 907-913. https://doi.org/10.1134/S0030400X19110274/7
39. E. D. Palik. Handbook of Optical Constants of Solids, Vol. 1. Academic Press, **1985**. https://doi.org/10.1016/C2009-0-20920-2
40. W. S. M. Werner, K. Glantschnig, and C. Ambrosch-Draxl. Optical constants and inelastic electron-scattering data for 17 elemental metals. *J. Phys. Chem. Ref. Data*, **2009**, *38*, 1013-1092. https://doi.org/10.1063/1.3243762
41. M. A. Ordal, R. J. Bell, R. W. Alexander, L. L. Long, and M. R. Querry. Optical properties of fourteen metals in the infrared and far infrared: Al, Co, Cu, Au, Fe, Pb, Mo, Ni, Pd, Pt, Ag, Ti, V, and W. *Appl. Opt.*, **1985**, *24*, 4493. https://doi.org/10.1364/ao.24.004493
42. J. M. Elazar, A. B. Djurišić, A. D. Rakić, and M. L. Majewski. Optical properties of metallic films for vertical-cavity optoelectronic devices. *Appl. Opt.*, **1998**, *37*(22), 5271-5283. https://doi.org/10.1364/ao.37.005271
43. H.-J. Hagemann, W. Gudat, and C. Kunz. Optical constants from the far infrared to the X-ray region: Mg, Al, Cu, Ag, Au, Bi, C, and Al_2O_3. *J. Opt. Soc. Am.*, **1975**, *65*, 742. https://doi.org/10.1364/josa.65.000742
44. P. B. Johnson and R. W. Christy. Optical constants of the noble metals. *Phys. Rev. B*, **1972**, *6*, 4370-4379. https://doi.org/10.1103/PhysRevB.6.4370
45. Inorganic Crystal Structure Database. Germany: FIZ Karlsruhe, https://icsd.products.fiz-karlsruhe.de/.

46. M. M. Shehata, A. M. Abdelreheem, S. A. Waly, and A. H. Ashour. Cu and Ag nanoparticles films deposited on glass substrate using cold cathode ion source. *J. Inorg. Organomet. Polym. Mater.*, **2017**, *27*, 720-727. https://doi.org/10.1007/s10904-017-0515-y
47. A. A. Solovyev, V. A. Semenov, V. O. Oskirko, K. V. Oskomov, A. N. Zakharov, and S. V. Rabotkin. Properties of ultra-thin Cu films grown by high power pulsed magnetron sputtering. *Thin Solid Films*, **2017**, *631*, 72-79. https://doi.org/10.1016/j.tsf.2017.04.005

PUBLISHER'S NOTE

Pleiades Publishing remains neutral with regard to jurisdictional claims in published maps and institutional affiliations.